

Determination of the Concentration Profile at the Surface of d-PS/h-PS Blends Using High-Resolution Ion Scattering Techniques

X. Zhao, W. Zhao, J. Sokolov,* and M. H. Rafailovich

Department of Physics, Queens College, Flushing, New York 11367

S. A. Schwarz and B. J. Wilkens

Bellcore, Red Bank, New Jersey 07701

R. A. L. Jones† and E. J. Kramer

Cornell University, Ithaca, New York 14853

Received January 25, 1991; Revised Manuscript Received May 6, 1991

ABSTRACT: Using the high-resolution ion profiling techniques of secondary ion mass spectrometry (SIMS) and time of flight forward recoil elastic scattering (TOF-FRES), we have measured the surface concentration profiles for a series of deuterated polystyrene (d-PS)/hydrogenated polystyrene (h-PS) blends as a function of deuterium volume fraction and annealing time. The data show that the profile is formed at a rate determined mostly by the bulk mutual diffusion coefficient. The form of the profile away from the surface ($Z > 100$ Å) is in agreement with predictions of current mean-field theories. On the other hand, in the near surface region ($Z < 100$ Å) a distinct flattening of the profile is observed, indicating that the short-ranged form of the interaction assumed in these theories may not be valid.

Introduction

A miscible polymer blend in contact with a surface is intrinsically an inhomogeneous system. The two components of the blend interact differently with the surface, and therefore the surface composition is usually not the same as the bulk. The equilibrium surface profile is determined by the balance between placement at the surface of the lower surface energy component and the cost of producing a composition gradient in the bulk. In the bulk (the region far away from the surface) where the effect of the surface vanishes, the blend approaches a homogeneous limit characteristic of the infinite system. In the ideal case where the interaction of the polymer chains with the surface is nonspecific (i.e., due to weak dispersion forces) the characteristic decay length of the surface concentration is expected to be on the order of R_g , the polymer radius of gyration. The most complete studies thus far on surface segregation have been done on the deuterated polystyrene/hydrogenated polystyrene (d-PS/h-PS) system. This system is an ideal model system where a small difference in the polarizability of the C-H and C-D bonds lowers the surface energy of the d-PS component and produces a small unfavorable bulk Flory interaction parameter, χ .¹ The surface excess of the d-PS component was first observed by Jones et al.² using the technique of forward recoil elastic scattering (FRES), and the decay for low bulk concentration was later probed by neutron reflectometry.³

Although the surface excess and long-range diffusion profiles that control the kinetics of segregation at long times can be readily studied by FRES, its poor depth resolution (~ 800 Å) precludes detailed measurements of the shape of either the nonequilibrium or equilibrium profile. On the other hand, neutron reflectivity, while very sensitive to the shape of the profile within the first

approximately 100 Å near the surface, is relatively insensitive to its longer range ($Z > 300$ Å) structure.

In order to accurately determine the shape of the concentration profile at the surface of the d-PS/h-PS blend and the dynamical factors involved in attaining equilibrium, we measured the composition at the surface of d-PS/h-PS blends using the techniques of secondary ion mass spectrometry (SIMS) and time of flight forward recoil elastic spectroscopy (TOF-FRES).⁴ Under the conditions described later, these techniques have resolutions of 115 and 250 Å, respectively, and the data are straightforward to interpret in a model independent way. The results can then be used to test the predictions of the mean-field theory.

Theoretical Background

Several authors⁵⁻⁷ have applied the mean-field formalism to investigate the phenomena of surface segregation in polymer blends. All the theories thus far are similar in that they assume a mean-field potential for the bulk and a Δ function (single monomer) interaction with the surface. With use of the notation of Schmidt and Binder,⁵ the total grand canonical free energy per unit area of a polymer blend, of concentration, ϕ , is given by

$$\frac{F[\phi(z)]}{k_B T} = \int_0^\infty dz \left[G(\phi) - \Delta\mu\phi + \frac{a^2}{36\phi(1-\phi)} \left[\frac{d\phi}{dz} \right]^2 + F_s \right] \quad (1a)$$

where $G(\phi)$ is the Flory-Huggins free energy

$$G(\phi) = \frac{\phi}{N_A} \ln \phi + \frac{1-\phi}{N_B} \ln (1-\phi) + \chi\phi(1-\phi) \quad (1b)$$

where $\Delta\mu = \partial G / \partial \phi$ is the chemical potential difference between the two components A and B, with polymerization indices N_A and N_B , respectively, " a " is the statistical segment length, and F_s is the "bare" surface free energy

* Present address: Cavendish Laboratory, Cambridge University, Madingley Road, Cambridge, CB3 0HZ U.K.

contribution. In order to solve eq 1 analytically, all treatments thus far make the approximation that F_s is a function only of the surface concentration, ϕ_1 , or equivalently that the interaction potential at the surface is a δ function. The validity of this approximation will be discussed later. This approximation has the advantage that the solution to the integral equation becomes insensitive to the exact functional form assumed for $F_s(\phi_1)$. It simply provides a boundary conditions for the segregation profile whose shape away from the surface is determined entirely by the bulk thermodynamic quantities, $G(\phi)$ and $\Delta\mu$.

Minimizing the functional of eq 1 yields the following solution to the concentration profile, $\phi(z)$, determined implicitly from

$$z = \frac{a}{6} \int_{\phi_1}^{\phi(z)} \frac{d\phi}{\sqrt{\phi(1-\phi)[G(\phi) - G(\phi_\infty) - \Delta\mu(\phi - \phi_\infty)]}^{0.5}} \quad (2)$$

where the integrand is only a function of the known bulk properties $\Delta\mu$ and ϕ_∞ . The surface concentration, ϕ_1 , does not affect the shape of the profile, since it appears only as the limit of the integral. From the boundary conditions that $\phi(z = \infty)$ is fixed at the bulk concentration, ϕ_∞ , and $\phi(z = 0)$ equals ϕ_1 , the following equation is obtained:

$$-\frac{dF_s(\phi_1)}{d\phi_1} = \frac{a}{3} \left[\frac{G(\phi_1) - G(\phi_\infty) - \Delta\mu(\phi_1 - \phi_\infty)}{\phi_1(1 - \phi_1)} \right]^{0.5} \quad (3)$$

The left-hand side of this equation yields the incremental bare surface energy saved by covering the surface with ϕ_1 , while the right-hand side is the incremental energy spent in establishing the segregation profile below the surface. Simultaneous solutions of the two sides of the equation for fixed ϕ_∞ yield the value of ϕ_1 , the surface concentration induced by the interactions at the polymer surface. In practice, $F_s(\phi_1)$ must be determined experimentally by measuring the surface concentrations for a range of ϕ_∞ values and evaluating the right-hand side of eq 3. This process is discussed further in a later section.

Experimental Section

The polymers used in this study were h-PS (Pressure Chemical Co.) and d-PS (Polymer Laboratories) of molecular weights 1.8×10^6 ($M_w/M_n < 1.3$) and 1.03×10^6 ($M_w/M_n < 1.15$), respectively. A series of blends with d-PS volume fraction, ϕ_∞ , ranging from 0.05 to 0.33 were prepared, and films 2–3- μm thick were spun-cast onto thin silicon wafers from toluene solutions. The samples were then sealed in glass ampules in a vacuum of 10^{-6} Torr and heated at 184°C for times ranging from 3 to 45 days. This temperature was chosen so as to be near the coexistence curve, but still in the one-phase region. The small-angle neutron scattering (SANS) experiments of Bates and Wignall⁸ measured $\chi = 0.20$ ($1/T - 2.4(4) \times 10^{-4}$), for a $\phi_\infty = 0.50$ blend of d-PS, and assuming negligible concentration dependence of χ , this yields for the molecular weights used in these experiments an upper critical solution temperature of 176°C and a critical d-PS concentration $\phi_c = 0.57$.

After annealing, the samples were examined by the technique of time of flight forward recoil elastic scattering (TOF-FRES). TOF-FRES is similar to the standard FRES technique⁴ except that the spatial resolution is improved by replacing the thick absorber foil used to stop the scattered α particles with a time of flight detector assembly (TOF) requiring only a thin foil to generate timing signals from passing ions. By simultaneously measuring the energy and transit time across a fixed gap for each particle, the device can discriminate electronically between the faster and lighter H and D ions and the slower α particles. For the typical FRES geometry, the energy resolution is about 15 keV, which translates into a depth resolution of approximately 250 Å for a polystyrene melt,^{9–11} as compared to 800 Å for FRES.¹⁰

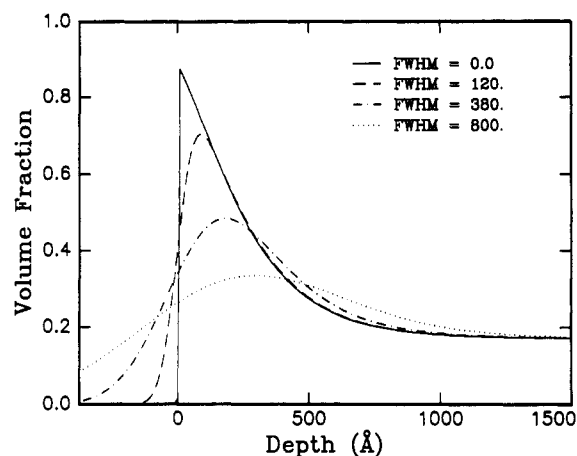


Figure 1. Effects of instrumental resolution (fwhm) on the determination of the shape of the concentration profile calculated from eq 2 for a $\phi_\infty = 0.21$ d-PS/h-PS blend: (—) theoretical result; (---) resolution of SIMS; (- · -) resolution of TOF/FRES; (···) resolution of FRES.

The effect of the experimental resolution in determining the surface segregation profile is shown in Figure 1. The solid line is the profile calculated from eq 2 for $\phi_\infty = 0.10$. The dotted line corresponds to the same curve convoluted by a Gaussian of full width half-maximum, fwhm = 800 Å, typical of the FRES resolution. From the figure it can be seen that, with this resolution, the shape of the profile is not resolved and only the total surface excess, Z^* , can be obtained. The shape of the profile becomes apparent after an improvement of the resolution by a factor of 2, and the decay length can be completely resolved when the resolution becomes 120 Å. Further improvement of the resolution, which would enable one to probe the very near surface region in the first 50 Å, is not currently possible with ion scattering techniques. In order to probe this region, neutron reflection is more appropriate.³

After TOF-FRES spectra are obtained, the samples were prepared for SIMS analysis, by floating onto their surface an additional 400-Å-thick PS film and evaporating a 60-Å-thick layer of gold on the whole assembly. No interfacial mixing between the components can occur in this process since both sample and coating films are in their glassy state. The purpose of the PS overlayer was to allow steady-state sputtering conditions to be established before the polymer blend surface region was exposed. The Au layer on the outermost surface provided a conducting path to ground in order to prevent charging of the nonconducting polymer film.

The sputtering was performed by using an Atomika 3000-30 ion microprobe and a 2-keV, 30-nA beam of Ar^+ ions at 30° off-normal incidence rastered over a 0.5-mm² region. Negative ions were monitored in order to avoid interference in the deuterium profile from H_2 radicals. This region was carefully chosen not to overlap with the previous beam spot from the TOF-FRES analysis. Occasionally an additional 1-keV defocused electron beam incident at 45° was directed onto the sample to eliminate beam-induced charging. The sputtering rate chosen for the above conditions was approximately 900 Å/h.

Analysis of SIMS

Figure 2 shows the raw SIMS data for a typical sample of d-PS volume fraction $\phi_\infty = 0.18$, annealed for 29 days. The ion masses analyzed correspond to carbon, CH, deuterium, and CD. From the data one first sees the narrow rise in the CH signal mirrored by a dip in D and CD signals, which corresponds to the thickness of the PS overlayer and defines the beginning of the sample surface. The large rise in the D and CD concentration, mirrored by the corresponding dip in the CH signal, is then apparent at the blend surface/overlayer interface. The carbon concentration is of course constant in all layers of the sample and was used as a monitor of the beam current.

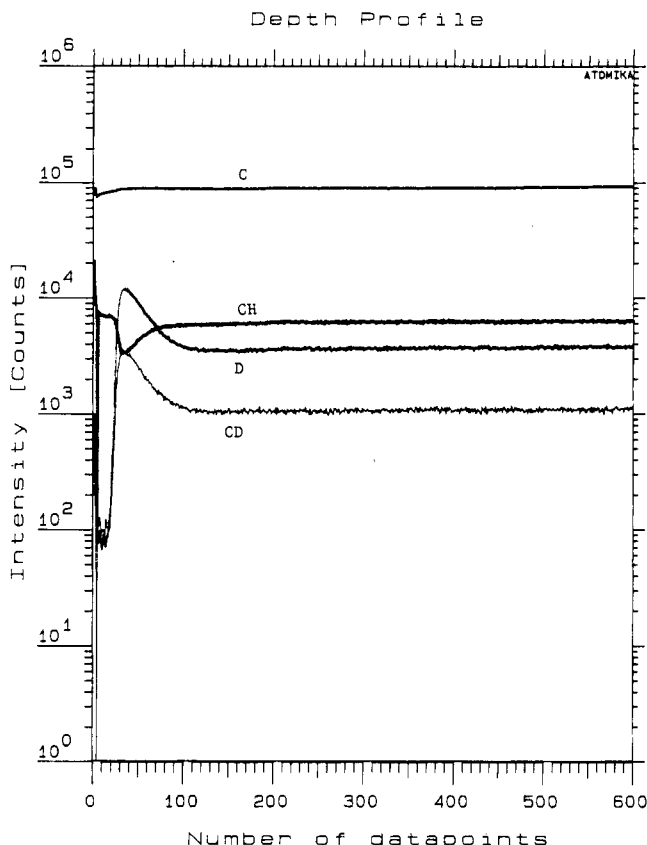


Figure 2. Raw SIMS data of a $\phi_{\infty} = 0.21$ d-PS sample annealed for 29 days. The data show scans for D, C, CH, and CD ions.

In this case, the flat carbon trace illustrates the stability of the sputtering beam over a 10-h period, the acquisition time of this spectrum.

In standard SIMS experiments the sputtering rate is directly converted to a depth scale by mechanically sensing the depth of the sputtered crater. This technique cannot be used with polymer films that are soft and therefore easily deformed. As a result the depth scale was calibrated by sputtering through a thin d-PS film, whose thickness of 560 Å was independently measured with FRES and ellipsometry. On the basis of this calibration, sputtering with the beam conditions described above yielded resolutions for the 14% to 86% rise and fall widths of 110 and 120 Å, respectively. As shown in Figure 1, this resolution allows the form of the concentration profile derived from mean-field theory in eq 2 to be probed.

Figure 3a shows TOF-FRES data from three samples annealed at 184 °C for 29 days with bulk volume fractions $\phi_{\infty} = 0.125$, 0.184, and 0.265. Figure 3b shows the SIMS data from the two lower concentration samples. The solid lines in both figures correspond to fits of eq 2 with three free parameters, ϕ_1 , ϕ'_{∞} , the effective bulk concentration in the near surface region, and χ . In all cases, best fits were obtained for $\chi = 1.50(3) \times 10^{-4}$, in good agreement with the value extrapolated from the results of Bates and Wignall,^{1,8} $\chi = 1.5(2) \times 10^{-4}$. The fit parameters as well as Z^* , the total surface excess, are tabulated in Table I and plotted in Figure 4. From Table I as well as Figure 4 it can be seen that SIMS yields the same (to within experimental error) results as the TOF-FRES technique, confirming that heavy ion sputtering from polymer films maintains a depth-independent rate over the region studied and reliable, quantitative, and reproducible results could be obtained. Furthermore, comparisons of parts a and b of Figure 3 indicates an additional important aspect of SIMS, namely, the improved signal-to-noise ratio, which

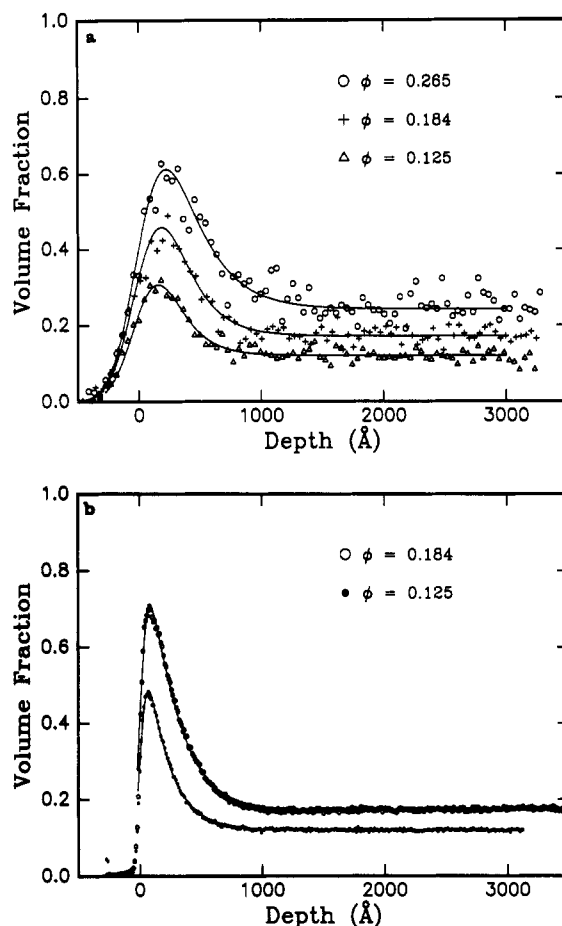


Figure 3. (a) TOF-FRES data from samples annealed at 184 °C for 29 days of initial volume fractions; (O) $\phi_{\infty} = 0.265$, (+) $\phi_{\infty} = 0.184$, (Δ) $\phi_{\infty} = 0.125$. The solid lines are fits to eq 2. (b) SIMS data from the (O) $\phi_{\infty} = 0.184$ and (\bullet) $\phi_{\infty} = 0.125$ samples. The solid lines are the best fit results of eq 2.

Table I
Summary of Results of SIMS and TOF-FRES
Measurements: Concentration Profiles of d-PS/PS Blends

ϕ_{∞}	ϕ'_{∞} ^a	ϕ_1 ^b	ϕ_1 ^c	Z^* , ^b Å	Z^* , ^c Å
0.005	0.0047	0.035 ± 0.004		3.8 ± 0.4	
0.025	0.024	0.15 ± 0.01		18.4 ± 3.7	
0.125	0.120	0.68 ± 0.01	0.69 ± 0.03	133 ± 4	136 ± 6
0.184	0.171	0.88 ± 0.01	0.87 ± 0.03	241 ± 8	238 ± 8
0.210	0.200	0.90 ± 0.01	0.90 ± 0.03	274 ± 9	275 ± 9
0.265	0.242		0.95 ± 0.03		364 ± 11

^a Volume fraction of d-PS at the depleted region next to the surface.

^b Result from the SIMS experiment. ^c Result from the FRES experiment.

allows the study of low-composition blends and detection of minor compositional fluctuations. But as seen from Figure 1 and discussed in refs 2 and 10, Z^* is still most quickly and efficiently measured by FRES. Consequently, the assumed calibration for all SIMS samples discussed in this work was checked by measuring Z^* independently with FRES.

Experimental Results

Plotting in Figure 4a Z^* vs ϕ_{∞} , we find the surface excess is directly proportional to ϕ_{∞} , with the proportionality constant of $K = 1075(23)$ Å. From Figure 4b it can be seen that ϕ_{∞} increases rapidly, with nearly full surface coverage by the d-PS component already occurring at $\phi_{\infty} \sim 0.10$. Hence, the linear increase in Z^* is then due mainly to the broadening of the decay profile with increasing ϕ_{∞} .

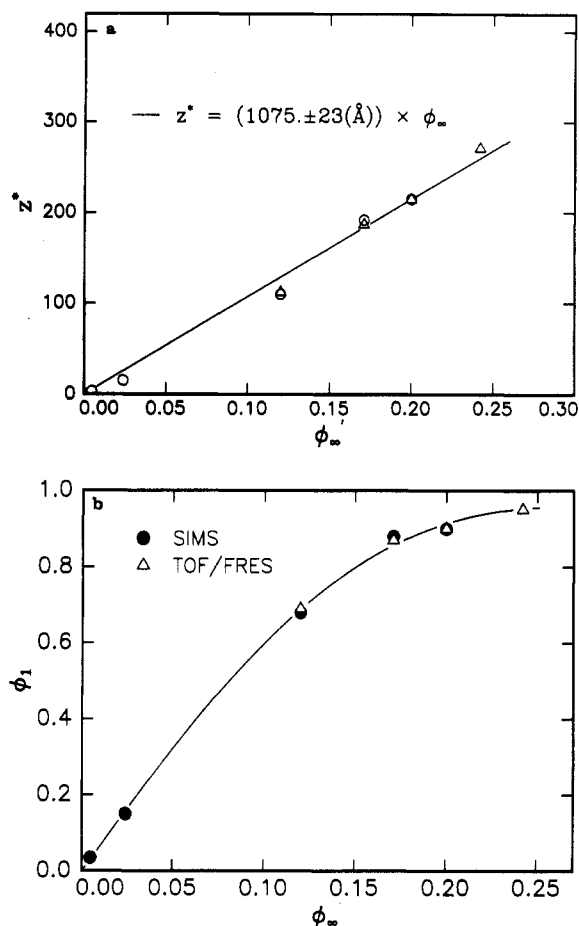


Figure 4. (a) Surface excess Z^* as measured by TOF-FRES (Δ) and SIMS (\circ) vs ϕ_∞ . (b) Surface concentration measured by TOF-FRES (Δ) and SIMS (\circ) as a function of ϕ_∞ .

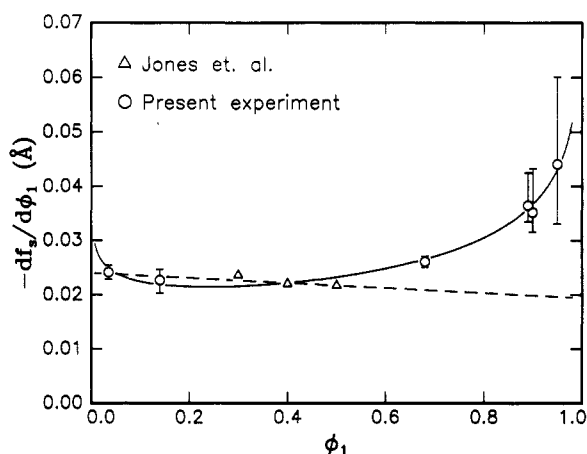


Figure 5. Derivative of the surface free energy as a function of the measured surface concentration. The dashed line corresponds to a fit using the linear approximation of ref 5, and the solid line corresponds to a fit with eq 5.

The increase in the decay length, λ , as ϕ_∞ approaches ϕ_c is predicted by eq 2 and was shown previously^{3,11} to coincide with the correlation length for density fluctuations in the bulk for $\phi_\infty < 0.10$. In Figure 4b we plot the measured surface concentration ϕ_1 as a function of ϕ_∞ . The solid line is drawn to guide the eye. In order to actually predict the dependence of ϕ_1 on ϕ_∞ , the solution to eq 3, $F_s(\phi)$ must be determined. In Figure 5 we plot the right-hand side of eq 3, for the experimentally measured values of ϕ_1 , and equate it to $dF_s(\phi_1)/d\phi_1$. From the dashed line in Figure 5 it can be seen that the empirical form assumed

by Schmidt and Binder,⁵ namely

$$F(\phi_1) = -\mu\phi_1 - g\phi_1^2 \quad (4)$$

where μ_1 and g are, respectively, the surface analogues of the chemical potential and χ , is only a good approximation to the data for small ϕ_1 . Including terms of order ϕ_1^3 did not significantly improve the fit.

The functional form that gave the best fit to the data is drawn as a solid line in Figure 5 and is given by

$$F(\phi_1) = -\mu_1\phi_1 + \alpha\phi_1 \ln \phi_1 + \beta(1 - \phi_1) \ln (1 - \phi_1) \quad (5)$$

with $\mu_1 = 0.027$ (5) \AA , $\alpha = 0.0030$ (7) \AA , and $\beta = -0.0095$ (\AA). This result is intuitively reasonable. The first term of this equation represents the chemical potential difference between the surface and bulk, which also appears phenomenologically in the formulations of Schmidt and Binder⁵ and Cohen and Muthukumar.⁷ The latter two terms are surface entropic factors, by analogy to the Flory-Huggins terms in eq 1.

Cohen and Muthukumar⁷ have recently derived a more realistic expression for $F_s(\phi_1)$, which includes a local surface interaction and surface entropy terms, as well as odd and even gradient terms to account for the intrinsic spatial asymmetry at the surface.

$$F_s(\phi_1) = -\mu_1\phi_1 + \alpha_1\phi_1 \ln \phi_1 + \beta_1(\phi_1) \ln (1 - \phi_1) + [\alpha_2 \ln \phi_1 + \beta_2 \ln (1 - \phi_1)](d\phi_1/dz) + \dots \quad (6)$$

has terms proportional to $(d\phi_1/dz)$ and $(d^2\phi_1/dz^2)$.

This expression has only three free parameters, μ_1 , C_A , and C_B , where $C_A - C_B$ is a term proportional to a surface χ . The α_i and β_i terms are complicated functions of C_A , C_B , N_A , and N_B . The first three terms of eq 6 coincide with the functional form that best fits our data. The main limitation of the theory, of both Cohen and Muthukumar⁷ and Schmidt and Binder,⁵ is the assumption of a short-ranged (δ function) surface interaction. The effect of taking the surface interaction to be strictly localized at the surface is to make the concentration profile, $\phi(z)$, simply "cut off" the bulk profile at some value ϕ_1 determined by the surface interaction parameters, which, in the case of Cohen and Muthukumar, yields unrealistically large values for the gradient terms in eq 6. Therefore, deviations of the shape of $\phi(z)$ from bulk behavior would provide clear evidence of the breakdown of the local interaction picture. This is indeed the case of large ϕ_1 , as is discussed further below.

Time Dependence of the Concentration Profile

Figure 6 shows the concentration profiles for a series of samples having $\phi_\infty = 0.33$ and annealed for times varying from 3 to 45 days. The solid lines are χ^2 fits to eq 2, and the results are summarized in Table II. ϕ'_∞ corresponds to the concentration in a depleted zone adjacent to the surface, as explained in ref 12, which from Figure 6 can be seen to be approximately 1000 \AA wide. This region is more clearly seen in Figure 7, where we plot the depth profile up to 4000 \AA from the surface of a $\phi_\infty = 0.21$ sample annealed for 29 days. Figure 8 is a plot of Z^* and ϕ_1 vs the square root of the annealing time for the profiles shown in Figure 6. As pointed out by Jones and Kramer,¹² conservation of mass requires that the excess material at the surface equal the amount missing from the near surface depleted region. It is reasonable to assume that sufficiently far from the surface the size of the depleted region should scale as $(Dt)^{1/2}$, where D is the bulk diffusion coefficient.

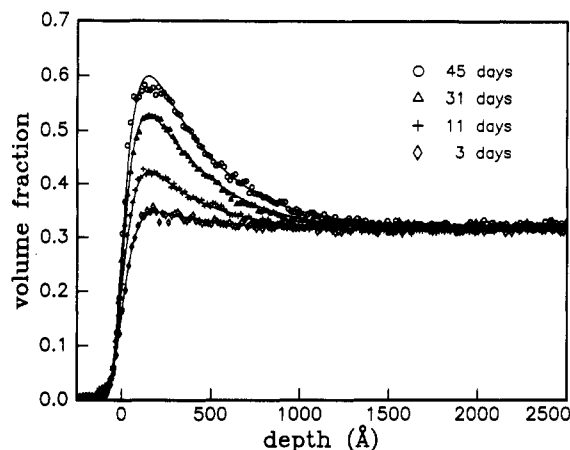


Figure 6. Surface concentration profiles for a $\phi_{\infty} = 0.33$ blend annealed for various times at $T = 184^{\circ}\text{C}$.

Table II
Summary of Results for the Concentration Profiles
Annealed for Different Times

t, h	ϕ_1	$Z^*, \text{\AA}$	ϕ'_{∞}
775.5	0.375	19.2	0.317
268.8	0.490	60.4	0.315
744.0	0.635	119.6	0.312
1080.0	0.700	163.0	0.320
infinite ^a	0.970	340	0.330

^a Predicted values for the equilibrium profile.

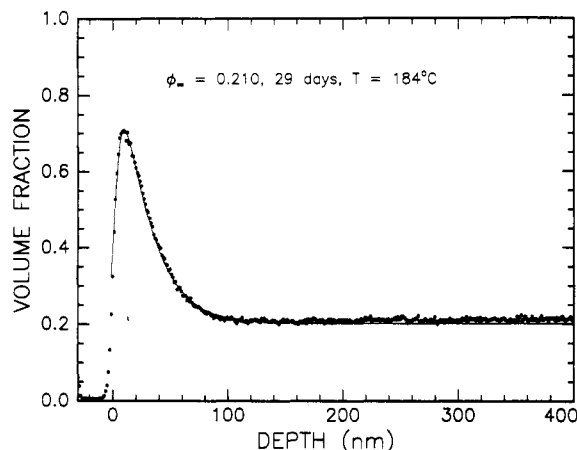


Figure 7. Surface concentration profile for a $\phi_{\infty} = 0.21$ blend annealed for 29 days at 184°C .

The surface excess can then be approximated by

$$Z^* = (\phi_{\infty} - \phi'_{\infty})(Dt)^{1/2} \quad (7)$$

From Tables I and II it can be seen that ϕ'_{∞} does not vary much from ϕ_{∞} for the measured annealing times. Taking an average value of $\phi'_{\infty} = 0.316$ from Table II together with the best fit value for the slope, $0.097 \text{ (5) } \text{\AA} \cdot \text{s}^{-1/2}$, of the Z^* curve, yields a mutual diffusion coefficient of $D = 4.83 \times 10^{-15} \text{ cm}^2/\text{s}$. This result is in good agreement with the mutual diffusion coefficient for a $\phi_{\infty} \sim 0.3$ blend at 184°C , $D = 3.0 \times 10^{-15} \text{ cm}^2/\text{s}$ calculated from the expressions given in the literature¹³ and using the measured value of $\chi = 1.50 \text{ (3) } \times 10^{-4}$. From Figure 6 and 8 one can see that all the profiles for the samples annealed less than 45 days are well fit by eq 2 and that ϕ_1 also scales as $t^{1/2}$ in the observed range of annealing times. This scaling indicates that the increase in the surface concentration, i.e., the adsorption to the surface, is not significantly faster than the bulk diffusion rate. Moreover, for each annealing time the profile of minimum energy is that consistent with the

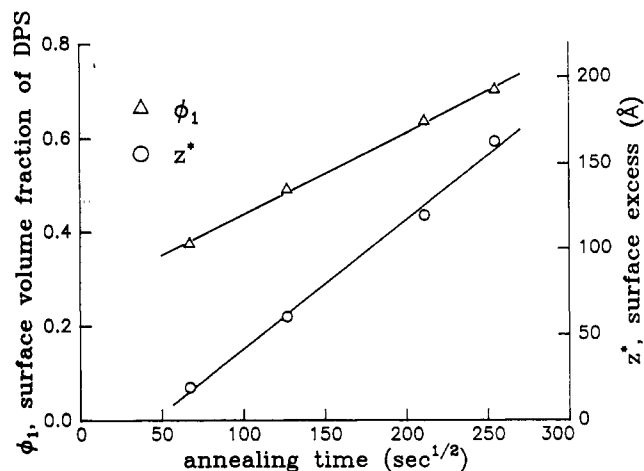


Figure 8. Measured surface concentration, ϕ_1 , and surface excess, Z^* , plotted as a function of the square root of the annealing time.

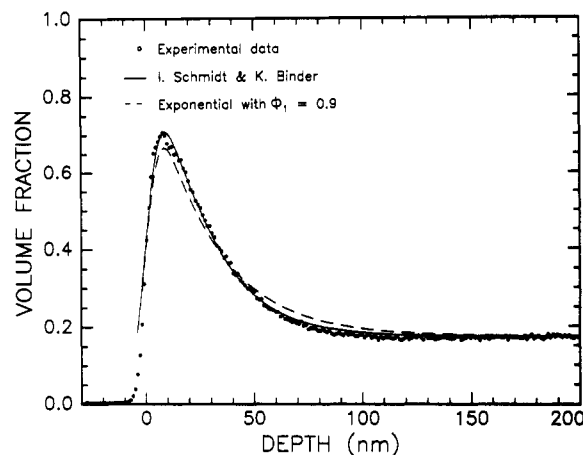


Figure 9. Concentration profile for a $\phi_{\infty} = 0.18$ d-PS/h-PS blend annealed for 29 days at 184°C . The solid line is a fit to eq 2, while the dotted line is a fit to an exponential decay.

mean-field prediction, with Z^* limited mainly by the bulk diffusion dynamics. Finally, the results show that the surface profile maintains a constant dynamic equilibrium with a depleted area where the concentration, ϕ'_{∞} , does not vary much from the bulk.

It must be stressed that no evidence exists as yet that these conclusions are generally true at short times. From the fact that the lines in Figure 8 do not go through the origin, we can infer that a short time Z^* builds up somewhat slower than predicted by eq 5.

Form of the Concentration Profile

We have previously shown that, for low ($\phi_{\infty} \sim 0.10$) d-PS volume fractions, the surface profile can be approximated by a simple exponential function with a decay length equal to the correlation length for concentration fluctuations in the bulk.^{3,11} It can be shown from eq 2 that in the framework of mean-field theory the profiles begin to differ significantly from a simple universal exponential decay at higher concentrations. This is illustrated in Figure 9, which shows the concentration profile for a $\phi_{\infty} = 0.18$ blend annealed for 29 days. From Figure 9 it can be seen that the spatial resolution of SIMS is sufficient to differentiate between an exponential decay and the mean-field functional form given by eq 2. On the other hand, the spatial resolution of SIMS is insufficient to determine the initial slope of the function, $d\phi/dZ$, in the near surface region. Neutron reflectometry³ on samples with $\phi_{\infty} < 0.15$ indicates that there may be a

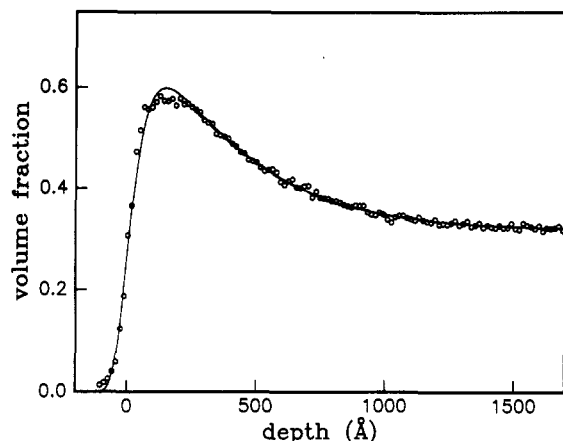


Figure 10. Expanded section of the near surface region for the $\phi_{\infty} = 0.33$ blend annealed for 45 days.

flattening of the concentration profile in the first 20 Å near the surface. A distinct flat region, approximately 100 Å wide, is clearly seen in Figure 10, which shows an expanded portion of the near surface region for the $\phi_{\infty} = 0.33$ sample annealed for 45 days. As can be seen from Table II, the Z^* for this profile is still far from equilibrium, and hence the width of the flat portion is just a lower limit on the final equilibrium value. The form of the profile in Figure 10 is not predicted by eq 2 but may still be consistent within the framework of the mean-field model, if one assumes a surface interaction of finite extent rather than the Δ function approximation used to solve eq 2 in closed form. Furthermore, eq 3 is a direct result of the Δ function surface boundary conditions,^{5,7} and therefore the form of the surface free energy obtained from eq 3 and shown in Figure 5 may not be correct for large ϕ_{∞} and ϕ_1 . It should be noted though that, as can be seen from Figure 10, the form of the decay of the surface concentration away from the surface layer is still consistent with eq 3 and, as mentioned previously, independent of the assumed form of the surface interaction.

From the time dependence data in Figure 6, it can be seen that the flat portion does not develop gradually or appear at large ϕ_1 , which would be expected if the surface potential were only a function of ϕ_1 . In fact, ϕ_1 for the profile in Figure 10 is smaller than that for other profiles where this feature is not as obvious. As ϕ_{∞} approaches the critical concentration, precise determination of the coexistence curve becomes more important. The experimental error on the value of χ for polystyrene¹ translates into a 10 °C uncertainty in the determination of the critical temperature for the blend. Hence, we cannot rule out the possibility that in the near surface region we are approaching a coexistence concentration and we are observing the growth of a surface macroscopic layer as predicted in

ref 5 and by eq 2. In order to differentiate between these two possibilities, further experiments are in progress by Jones et al.¹⁴ on the better characterized system PEP/d-PEP and by Schwarz et al.¹⁵ on the PS/PBrS system where this type of surface layering has been observed.

Conclusions

In conclusion, we have demonstrated that the spatial resolution obtained by a combination of ion scattering techniques is sufficient to determine the form of the concentration profile at the surface of a polymer blend. The shape of the profile is consistent with mean-field theories except in the near surface region where the gradient is much smaller than predicted, indicating that the surface interaction is longer ranged than assumed in the strictly local interaction models. The growth of the decay profile, as well as the surface concentration, seems to be a diffusion-limited process, with a diffusion constant equal to the bulk mutual diffusion coefficient.

Acknowledgment. We thank Prof. M. Muthukumar for many helpful discussions and Dr. K. W. Jones for the use of the BNL 3.0 MeV Van de Graaf facility (under DOE Contract No. DE-AC02-76CH00016). This work was supported in part by the National Science Foundation (Polymer Program Grant No. DMR-8921556), the Department of Energy (Contract No. DE-FG02-90ER45437), and the donors of the Petroleum Research Fund, administered by the American Chemical Society.

References and Notes

- (1) Bates, F. S.; Wignall, G. D. *Phys. Rev. Lett.* **1986**, *57*, 1429.
- (2) Jones, R. A. L.; Kramer, E. J.; Rafailovich, M. H.; Sokolov, J.; Schwarz, S. A. *Phys. Rev. Lett.* **1989**, *62*, 280.
- (3) Jones, R. A. L.; Norton, L. J.; Kramer, E. J.; Composto, R. J.; Stein, R. S.; Russell, T. P.; Mansour, A.; Karein, A.; Felcher, G. P.; Rafailovich, M. H.; Sokolov, J.; Zhao, X.; Schwarz, S. A. *Europhys. Lett.* **1990**, *12*, 41.
- (4) Sokolov, J.; Rafailovich, M. H.; Jones, R. A. L.; Kramer, E. J. *Appl. Phys. Lett.* **1989**, *54*, 590.
- (5) Schmidt, I.; Binder, K. *J. Phys.* **1985**, *46*, 1631.
- (6) Nakanishi, H.; Pincus, P. *J. Chem. Phys.* **1983**, *79*, 977.
- (7) Cohen, M. S.; Muthukumar, J. M. *J. Chem. Phys.* **1989**, *90*, 10.
- (8) Bates, F. S.; Wignall, G. D. *Macromolecules* **1986**, *19*, 932.
- (9) Mills, P. J.; Green, P. F.; Palmstrom, C. J.; Mayer, J. W.; Kramer, E. J. *Appl. Phys. Lett.* **1984**, *45*, 957.
- (10) Kramer, E. J. *Phys. B*, to be published.
- (11) Rafailovich, M. H.; Sokolov, J.; Zhao, X.; Jones, R. A. L.; Kramer, E. J. *Hyperfine Interact.* **1990**, *62*, 45.
- (12) Jones, R. A. L.; Kramer, E. J. *Philos. Mag.*, in press.
- (13) Green, P. F.; Doyle, B. L. *Phys. Rev. Lett.* **1986**, *57*, 2407. Green, P. F.; Kramer, E. J. *J. Mater. Res.* **1986**, *1*, 202.
- (14) Jones, R. A. L.; Norton, L. J.; Kramer, E. J.; Bates, F. S.; Wiltzius, P. *Phys. Rev. Lett.* **1991**, *10*, 1326.
- (15) Schwarz, S. A.; et al. *Polymeric Alloys*; MRS: 1991; in press.
- (16) Zhao, X.; et al. *Bull. Am. Phys. Soc.*, in press.

Registry No. h-PS, 9003-53-6; d-PS, 27732-42-9.